Pushing the boundaries of chemistry? It takes #HumanChemistry

Make your curiosity and talent as a chemist matter to the world with a specialty chemicals leader. Together, we combine cutting-edge science with engineering expertise to create solutions that answer real-world problems. Find out how our approach to technology creates more opportunities for growth, and see what chemistry can do for you at:

evonik.com/career

EVONIK
Leading Beyond Chemistry

Materials in Organic Electrochemical Transistors for Bioelectronic Applications: Past, Present, and Future

Maximilian Moser,* James F. Ponder Jr., Andrew Wadsworth, Alexander Giovannitti, and Iain McCulloch

Organic electrochemical transistors are bioelectronic devices that exploit the coupled nature of ionic and electronic fluxes to achieve superior transducing abilities compared to conventional organic field effect transistors. In particular, the operation of organic electrochemical transistors relies on a channel material capable of conducting both ionic and electronic charge carriers to ensure bulk electrochemical doping. This review explores the various types of organic semiconductors that are employed as channel materials, with a particular focus on the past 5 years, during which the transducing abilities of organic electrochemical transistors have witnessed an almost tenfold increase. Specifically, the structure–property relationships of the various channel materials employed are investigated, highlighting how device performance can be related to functionality at the molecular level. Finally, an outlook on the field is provided, in particular toward the design guidelines of future materials and the challenges ahead in the field.

1. Introduction

Bioelectronics is enabled by the transduction of electronic signals into biological ones and vice versa.[1] Although the vast majority of articles in the literature have credited Luigi Galvani, with the twitching frog experiment, as the father of bioelectronics, Plato's Meno suggests that the electrogenic properties of electric rays have been known and used for the wellbeing of the Greek population for over 2000 years.[2,3] Currently, bioelectronic devices are predominantly found in healthcare

applications and include neural interfacing electrodes, cochlear implants, glucose sensors for diabetics, and many more.[4–9]

Over the last two decades the field has experienced rapid growth, as shown in **Figure 1**, which collates the total number of citations of publications which include the term "bioelectronics" between 1999 and 2017. A large contribution to this rise stems from the increased research activity in the broader context of organic electronics. There, significant advances in the mechanistic understanding and materials design for organic field effect transistors (OFETs),[10–14] organic light emitting diodes (OLEDs),[15–17] electrochromic displays (ECDs),[18] charge storage devices,[19] and organic photovoltaics (OPVs)[20–23] have spurred further development. A common feature of the materials used for these various applications lies in the delocalized nature of conjugated, π-electrons, giving rise to semiconducting bandgaps, and facilitating charge carrier mobility along and between chains. While the electrical properties of the materials used can be easily tailored by chemical design, another approach is chemical doping. Here, the addition of a dopant either removes electrons (p-type doping) from the highest occupied molecular orbital (HOMO) or donates electrons (n-type doping) to the lowest unoccupied molecular orbital (LUMO) to afford conductive polaron or bipolaron states. This oxidation or reduction process can also be achieved electrochemically, when application of a potential between electrodes inject or extract charges from the semiconductor and the electrolyte.

The predominant use of organic semiconductors, rather than their inorganic counterparts, as translators between the electronic and biological domains arises from a unique set of features possessed by these materials, the most crucial of which being the weak van der Waals' intermolecular forces conferring organic materials a "soft" character.[2] This softness can be further enhanced through the choice of the polymer's side groups, which can further facilitate the swelling of the material allowing for the uptake of both ions and solvent throughout the bulk during the electrochemical doping and dedoping process. This results in an efficient ion-to-electron signal conversion. A simple and elegant demonstration of this phenomenon is the "moving front" experiment, which also found ionic mobility in conductive polymers to be of a similar magnitude as those in
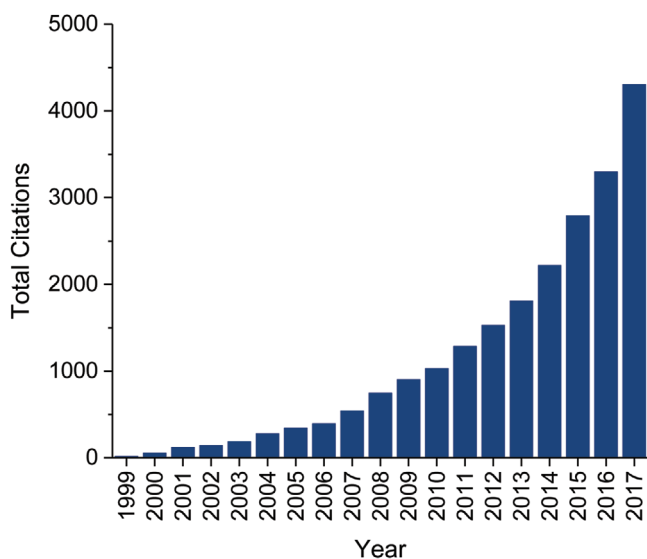
M. Moser, Dr. J. F. Ponder Jr., Dr. A. Wadsworth, Dr. A. Giovannitti
Department of Chemistry and Centre for Plastic Electronics
Imperial College London
London SW7 2AZ, UK
E-mail: maximilian.moser13@imperial.ac.uk
Prof. I. McCulloch
Department of Chemistry and Centre for Plastic Electronics
Imperial College London
London SW7 2AZ, UK
Prof. I. McCulloch
King Abdullah University of Science and Technology (KAUST)
Physical Sciences and Engineering Division
KAUST Solar Center (KSC)
Thuwal 23955-6900, Saudi Arabia

**ADVANCED
SCIENCE NEWS**
www.advancedsciencenews.com

**ADVANCED
FUNCTIONAL
MATERIALS**
www.afm-journal.de

Figure 1. Total number of citations of publications including the term "bioelectronics" from 1999 to 2017. Data obtained from Web of Science.

water.[24] Additional benefits of organic semiconductors over their inorganic counterparts include their: i) facile chemical modification, allowing functionality to be defined at the molecular level; ii) solution processability, enabling low temperature and low-cost processing; iii) compatibility with conventional printing and roll-to-roll techniques, facilitating their industrial scale up and application; iv) low operating voltages, allowing for operation in aqueous solvents and reducing the likelihood for potential side reactions; and v) high potential for biocompatibility, which can be further increased by tuning the self-assembling properties of the material or by incorporation of biomolecular side groups.[25–28]

Since the inception of modern bioelectronics, numerous device types, and architectures have been developed and employed for various applications. Amongst these are: electrodes for cell culture and neural recording, OFETs targeted for gas sensing, organic electrochemical transistors (OECTs) for signal amplification and analyte sensing as well as many others.[29–33] In this review, we report the significant progress made in OECT technology over the last few years, with a particular focus on the channel materials employed. More detailed accounts of alternative devices in bioelectronics; OFETs as sensing elements in bioelectronics, and the various biological applications of OECTs can be found elsewhere in the literature.[25,34,35] Additionally, as OECTs are primarily of interest in regards to biological systems, this review focuses on OECTs using aqueous electrolytes, although, OECTs using organic electrolytes or mixed organic/aqueous electrolytes are also being investigated.[36–38]

2. OECT Operating Principles and Performance

Similar to electrolyte gated-OFETs (EG-OFETs), OECTs feature a three-terminal architecture comprising a source, drain, and gate electrode. The gate electrode is placed into contact with the channel material via an electrolyte, illustrated in **Figure 2**.

Maximilian Moser received his M.Sc. degree in Chemistry from Imperial College London in 2017, during which he focused on the design of small molecule nonfullerene acceptors for organic photovoltaics. Since then, he has embarked on his Ph.D. at the Centre for Plastic Electronics at Imperial College London under the supervision of Prof. Iain McCulloch. His current research interests are focused on the development of novel materials for bioelectronic applications including organic electrochemical transistors and ion sensors.

James Ponder received his B.Sc. degree from the University of North Florida in 2011. He then joined the research group of Prof. John R. Reynolds at the Georgia Institute of Technology (GaTech). During his time there, James studied redox active polymers for electrochromic and charge storage applications as well as polymer thermoelectrics. In 2017, James received his Ph.D. from GaTech and joined the research group of Prof. Iain McCulloch as a postdoctoral researcher. He is currently designing materials for spintronics and bioelectronics in addition to nonfullerene acceptors for organic photovoltaics.
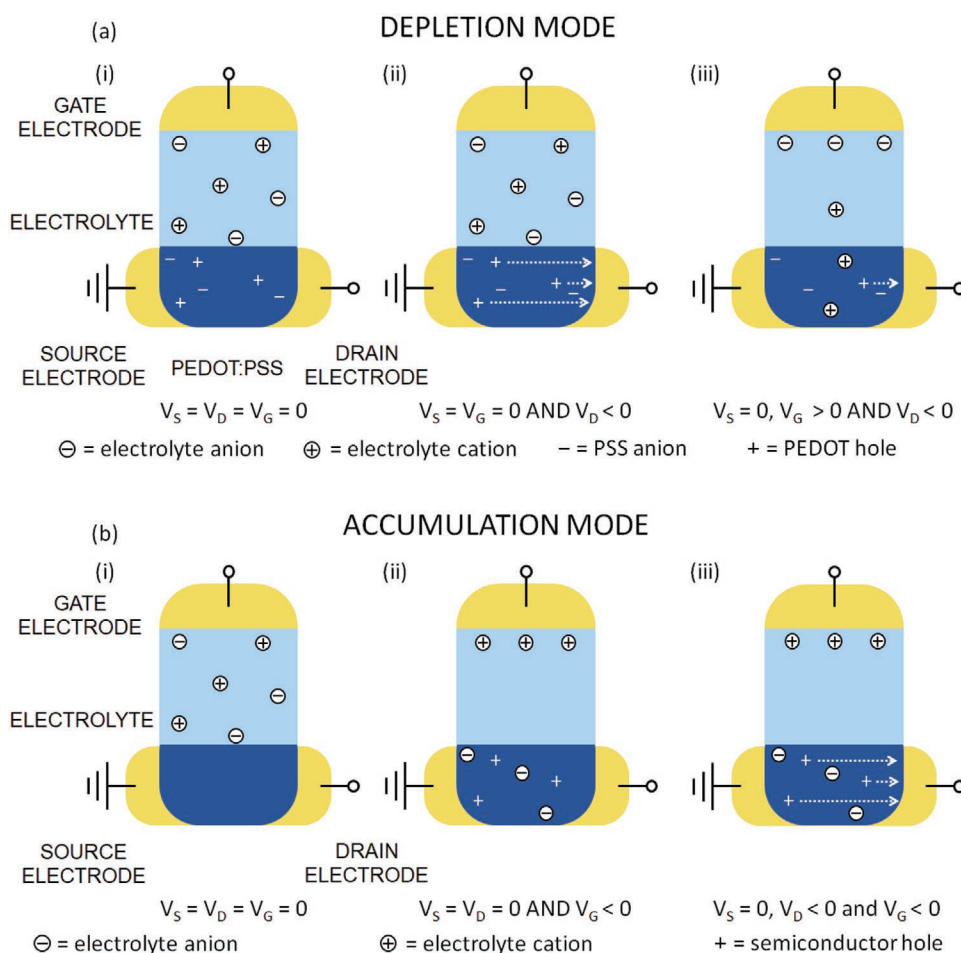
Iain McCulloch holds positions as Professor of Chemical Science within the Division of Physical Sciences and Engineering of KAUST, and a Chair in Polymer Materials within the Chemistry Department at Imperial College London. He is also the Director of KAUST Solar Center and a cofounder and director of Flexink Limited. Previously, he spent 18 years managing industrial research groups at Hoechst Corporation in the US and Merck in the UK, focused on understanding the control of microstructure and energy levels in conjugated aromatic semiconducting molecules.

As in EG-OFETs, changes in the source–drain current (I_{SD}) can be modulated by changes in the gate voltage (V_G) as this varies

ADVANCED
SCIENCE NEWS
www.advancedsciencenews.com

ADVANCED
FUNCTIONAL
MATERIALS
www.afm-journal.de

Figure 2. Device architecture and operating principle for a) a depletion mode OECT based on **PEDOT:PSS** i) in its unbiased state, ii) with hole flow toward the drain electrode, and iii) reduced hole flow toward the drain electrode upon application of a positive gate voltage; b) an accumulation mode OECT using a p-type channel material i) in its unbiased state, ii) after electrochemically doping the channel by the application of a negative gate voltage, and iii) with hole flow toward the drain electrode upon application of a negative potential at both the drain and gate electrode.

the doping level of the channel material. The key difference between EG-OFETs and OECTs results from the changes in the doping level being restricted to the channel–electrolyte interface for EG-OFETs, while in OECTs the variation in the doping level is observed throughout the bulk of the channel. Consequently, judicious material selection and device configuration in OECTs can lead to superior signal amplification properties in OECTs.[39]

OECTs can be subdivided into four categories, depending on their p or n-type charge transporting properties and on their accumulation or depletion mode of operation. In accumulation mode devices, the organic semiconductor is poorly conductive in its unbiased state and requires application of a gate potential to be doped, resulting in increased conductivity through the channel material, see Figure 2. Conversely, for depletion mode OECTs the organic semiconductor is conductive, and often self-doped, in its unbiased form and application of a gate potential leads to electrochemical dedoping, leading to a reduction of conductivity through the channel material. The operating principle of a depletion mode OECT using poly(3,4-ethylenedioxythiophene):poly(styrenesulfonate) (**PEDOT:PSS**)

as a model channel material is illustrated in Figure 2. The electron-donating nature of the 3,4-dioxyalkyl bridge on the thiophene moieties yields a highly electron-rich **PEDOT** backbone, thus giving rise to the p-type character of **PEDOT:PSS**. As the **PEDOT** backbone is partially oxidized, with sulfonate groups in PSS providing charge balance, it operates in depletion mode. By applying a negative potential at the drain electrode (V_D) while maintaining zero potential at the source (V_S) and gate electrodes, the holes located along the **PEDOT** backbone are swept across the channel. Increasing the V_G causes anions in the electrolyte to migrate toward the gate electrode, forming an electrical double layer. Concomitantly, cations are injected from the electrolyte into the channel material thereby progressively charge balancing the PSS anions and dedoping the **PEDOT** backbone, thereby depressing the source–drain current and eventually turning the device "off." As a result of the bulk electrochemical doping/dedoping process, which according to the Bernards model is ascribed to an ionic and electronic component, mobility measurements in OECTs are not straightforward.[40] OECT performance is thus typically ascribed by another metric, the transconductance (g_m), defined

**ADVANCED
SCIENCE NEWS**
www.advancedsciencenews.com

**ADVANCED
FUNCTIONAL
MATERIALS**
www.afm-journal.de

mathematically in Equation (1). To link g_m to material relevant parameters from experimental data, g_m can also be expressed as Equation (2). From this equation it follows that the g_m of an OECT can be modulated by adjusting either the channel dimensions (w, d and l) or the channel material employed (μ and C^*). Additionally, the g_m of OECTs has also been shown to be strongly dependent on the nature of the gating electrode.[41–44]

$$g_m = \frac{\partial I_{SD}}{\partial V_G} \qquad (1)$$

$$g_m = \frac{wd}{l}\mu C^*\left(V_{Th} - V_G\right) \qquad (2)$$

where ∂I_{SD} = change in current between the source and drain electrodes, ∂V_G = change in voltage between the gate and source electrodes, w = channel width, d = channel thickness, l = channel length, μ = charge carrier mobility, C^* = volumetric capacitance, V_{Th} = threshold voltage, and V_G = gate voltage.

In addition to the g_m of OECTs, variables such as OECT switching times, on–off ratios, and stability must also be taken into consideration for a more comprehensive picture of OECT performance. Switching times are commonly employed to measure the transient response of devices and are usually obtained by measuring the I_{SD} as a function of time upon the application of square-wave gate voltages. On (τ_{ON}) and off (τ_{OFF}) times are then defined as the time required to reach 90% and 10% of the I_{SD} for fully switched on and off devices, respectively.[45] A limitation of reporting τ_{ON} and τ_{OFF} values is that both are directly proportional to the channel dimensions, in particular channel thickness. Care must therefore be taken when comparing τ_{ON} and τ_{OFF} values between various devices and ideally should always be performed for equally sized channels. High on–off ratios are preferred as this allows for higher sensitivity. Lastly, device stability is also of utmost importance, especially in the context of in vivo applications of OECTs. A common procedure for OECT stability evaluation involves measuring the I_{SD} of devices over several hours by application of either a constant or more commonly a pulsed applied voltage load.[25] The figure of merit here is the percentage of the initial I_{SD} retained after extended voltage cycling.

Although the performance of the various channel materials is determined entirely from the previously mentioned parameters, additional insights into the properties of a channel material can be gained through a range of alternative analytical techniques, including those commonly encountered in the fields of OFETs, OPVs and electrochromics, such as: i) cyclic voltammetry (CV), ii) grazing incidence wide-angle X-ray scattering, iii) transistor mobility, iv) electrochemical impedance spectroscopy, and v) spectroelectrochemistry. In the context of OECTs, spectro-electrochemical measurements are particularly useful, as they enable simultaneous acquisition of spectroscopic and electrochemical information, and provide an indication of how effectively a polymer film is doping via uptake of solvated ions. Although there is no standard setup in spectroelectrochemistry, a typical measurement configuration consists of a transparent conductive electrode, usually indium-tin oxide (ITO), coated with the material of interest.[46] This electrode is then placed in an electrolyte solution and coupled to counter and reference electrodes within the sample holder of a spectrophotometer. During spectroelectrochemical cycling, the electrochromic properties of the material are evaluated by probing its absorption as a function of applied potential. In the case of **PEDOT** as a model system, application of increasingly positive potentials leads to progressive doping of the **PEDOT** film, resulting in the appearance of a polaronic absorption band around 900 nm and concomitant extinction of the shorter wavelength π–π^* absorption band followed by bleaching of the polaronic absorption and appearance of a bipolaron band, as shown in **Figure 3**.

3. p-Type OECT Channel Materials

Typically, the channel in OECTs consists of a semiconducting or conducting organic polymer. These can be synthesized either electrochemically or chemically. In the electrochemical approach the monomer, dopant and electrolyte are dissolved in a common solvent and placed in a conventional three-electrode
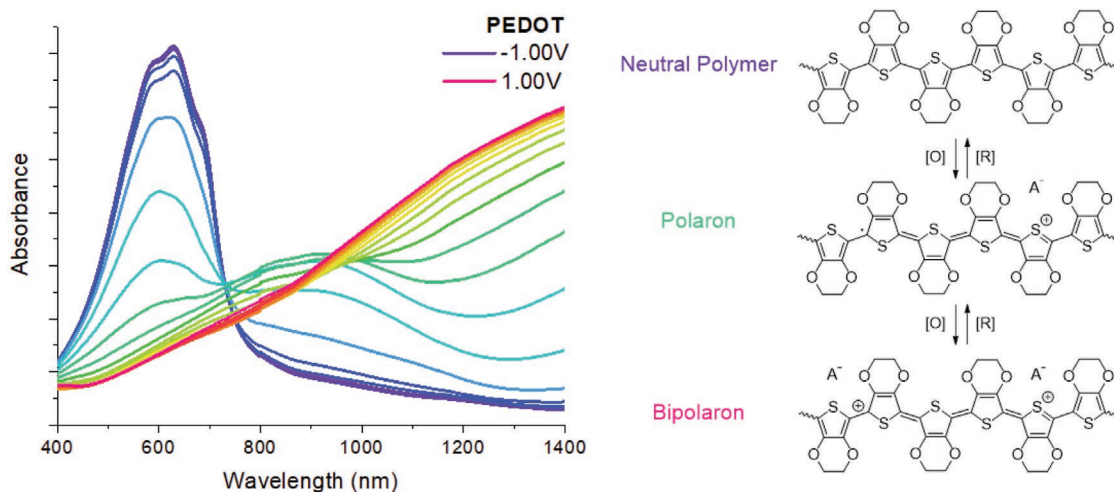
Figure 3. a) Spectroelectrochemistry of electropolymerized **PEDOT** on ITO glass in an organic electrolyte upon the application of a voltage from −1.0 V to +1.0 V in 0.1 V increments and b) mechanistic explanation of the electrochemical doping/dedoping process.

cell. Upon application of an electrochemical potential to the working electrode, monomers in solution at the working electrode are oxidized, affording a positively charged radical, which can further react with another monomer ultimately leading to the deposition of a polymer film that is tightly adhered to the electrode.[47,48] Examples of reductive electropolymerization, in which reduction of the monomer at the working electrode occurs prior to reaction with another monomer, have also been reported in the literature, however much less frequently.[49–51] By tuning various parameters, including the deposition method (e.g., CV or potentiostatic/galvanostatic methods), the nature of the working electrode, monomer concentration, electrolyte, and solvent, suitable polymer films can be obtained.[52] An advantage of this technique is the close control over the channel thickness that can be obtained by altering details of the deposition.[53] The most limiting aspects of the electrochemical deposition method are: i) its limited scope for monomer choice, allowing for the polymerization of only a handful of substrates, ii) its lack of control over copolymer sequencing, and iii) the prerequisite of a conductive surface on which to grow the polymer film, a difficult feature to implement in OECTs.[54,55]
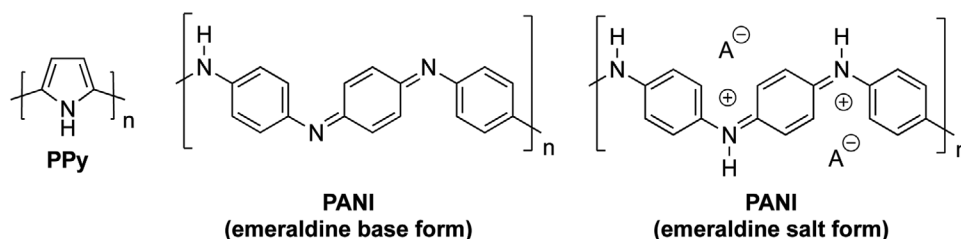
The solution-phase chemical approach typically involves the synthesis of the relevant monomers, followed by a polymerization step utilizing either oxidative or transition metal catalyzed crosscoupling polymerization conditions.[32,56] A key advantage of these chemical approaches are the numerous routes and monomer choices that are available to synthetic chemists to afford the desired polymer. Nonetheless, care must be taken when selecting the reaction conditions, especially if the resulting channel material is to be used in contact with biological systems, as polymers may contain residual monomers, solvents, metals,[57] etc., which can be highly toxic for living systems.
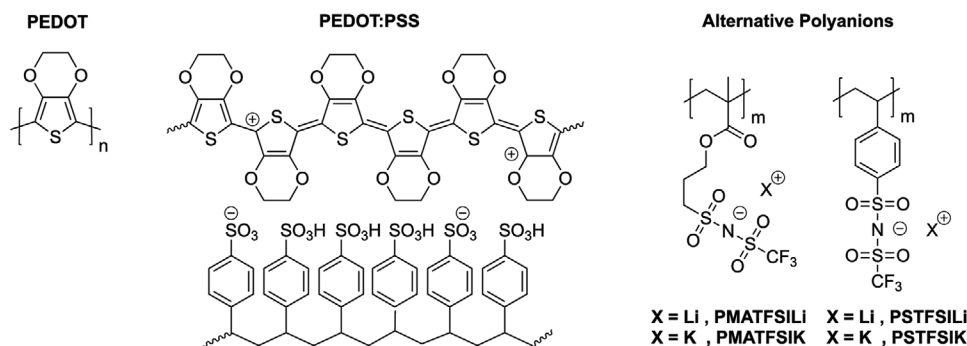
3.1. Early Channel Materials

Amongst the first materials employed as the channel were polypyrrole (**PPy**) and polyaniline (**PANI**), structurally shown in **Figure 4**. Anodically electropolymerized **PPy** onto gold electrodes was the first channel material to be implemented in an OECT.[47] In this device, a V_G of −0.2 V had to be applied relative to a standard calomel electrode to switch off the device, as this coincided with the oxidation potential of **PPy**. At more positive values of V_G, the device turned on and reached a maximum g_m of ≈0.1 mS at a V_G of +0.1 V, while τ_{ON} was ≈10 s (for a channel w and l of 1.4 µm) and the on–off ratio was 3000. The deployment of **PPy** in OECTs has since been scarce, predominantly due to its oxidative instability, as the doped polymer has a propensity to

crosslink, thus rendering devices inoperable.[47] One of the few examples in literature employing **PPy** as the active layer material was in an OECT-based penicillin sensor, in which penicillinase was immobilized onto **PPy**.[58] Here, as a result of the enzymatic action of penicillinase, penicillin was converted into penicilloic acid resulting in a change in the local pH, thus increasing **PPy**'s conductivity and correspondingly the I_{SD}.

To overcome the limitations posed by **PPy**, alternative semiconducting polymers have been investigated as channel materials, leading to **PANI**-based OECTs. **PANI** was originally chosen as a suitable material for OECTs due to its similar conductivity to **PPy** (up to ≈10^2 S cm^{-1}), superior stability in electrolytes, ease of synthesis and lower-cost starting materials.[59–61] Early work on **PANI**-based OECTs revealed significantly improved stability with devices retaining up to 80% of their initial I_{SD} while cycling devices over 10 h.[48] In combination with higher transconductances of 0.4 mS at +0.15 V and faster switching times approaching ≈50 ms and <50 ms for τ_{ON} and τ_{OFF}, respectively (for a channel w and l of 1.7 µm and d of 5 µm), **PANI** devices represented a significant improvement compared to the previously developed **PPy** ones. In the same set of studies, qualitative chemical sensing experiments were also performed by evaluating the responsive behavior of the I_{SD} upon pH increments. Here, increases in the pH from 1 to 6 resulted in a markedly lower I_{SD}, which was due to the chemical dedoping of **PANI**'s highly conductive emeraldine salt form to the poorly conducting emeraldine base form, which has been reported to occur at a pH of 5.5.[62] While this feature suggested the potential applicability of **PANI**-based OECTs as pH sensors, the original I_{SD} values could not be restored when returning to pH 1, thus highlighting the irreversibility of the system. Consequently, a drawback of **PANI** as channel material is its requirement of a low operating pH, hence limiting its applicability for biologically relevant sensing, which often occurs at physiological pH. Nonetheless, **PANI**-based OECTs have still been successful as chemical sensors, in particular with outer-sphere redox reagents, whereby addition of either an oxidant, $Fe(CN)_6^{3+}$, or reductant, $Ru(NH_3)_6^{2+}$, was shown to turn devices on and off, respectively. In another report **PANI**-based OECTs have also been used as biosensors.[63] Here glucose oxidase, which is stable down to a pH of 5, was immobilized in a poly(1,2-diaminobenzene) film and deposited onto a **PANI** channel. To link the enzymatic action to the semiconducting polymer a tetrathiafulvalene redox shuttle was employed. Consequently, this device setup enabled glucose sensing down to 4×10^{-6} M. Further optimization in the device setup, in particular tuning of the channel dimensions, resulted in a significantly improved sensitivity down to 2×10^{-6} M.[64]

Figure 4. Chemical structures of the various early OECT channel materials.

**ADVANCED
SCIENCE NEWS**
www.advancedsciencenews.com

**ADVANCED
FUNCTIONAL
MATERIALS**
www.afm-journal.de

Figure 5. Representative chemical structures of **PEDOT** and various **PEDOT** derivatives including **PEDOT:PSS** and alternative polyanions.
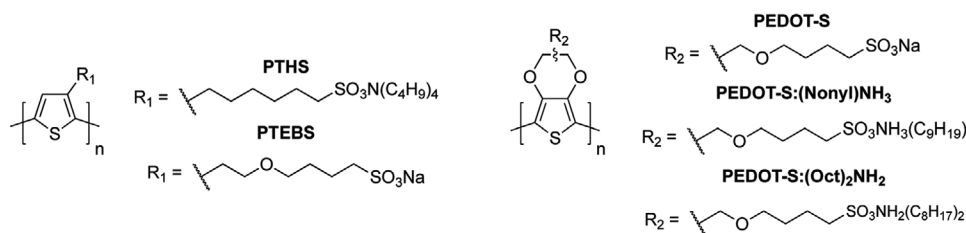
3.2. PEDOT Derivatives and Conjugated Polyelectrolytes

Since its first use in OECTs, **PEDOT:PSS**, has emerged as the most successful material for OECT applications and is still widely considered as the golden standard. Although originally intended as an antistatic agent, it has also been employed in a wide range of fields including electrochromics displays, organic thermoelectrics, and organic photovoltaics as a buffer layer or transparent conductive electrode.[65–72] While the precise structure of **PEDOT:PSS** is dependent on the **PEDOT** doping level, which is controlled by use of additive and post film casting treatments, **Figure 5** serves as a representative structure of highly p-doped **PEDOT:PSS**. **PEDOT:PSS** was first introduced as channel material in 2002.[73] In this context, **PEDOT:PSS** was chosen in particular due to its widespread commercial availability and significantly higher electrical conductivity, which can reach up to ≈3000 S cm^{-1} depending on processing and treatments,[74] compared to **PPy** and **PANI**.[73] Additionally, **PEDOT** and **PEDOT:PSS**, along with derivatives of these materials, have been utilized as charge storage materials due to their broad electroactive responses and high volumetric capacitances.[75–78] This combination of high charge transporting, charge storage capabilities, and widespread availability made **PEDOT:PSS** an ideal material for OECT research. Indeed, devices based on **PEDOT:PSS** demonstrated a g_m approaching 1.2 mS, τ_{ON} and τ_{OFF} of 0.5 and 0.02 s respectively (for a channel w of 200 µm) and on–off ratios in excess of 10^5. Processability was also improved as the devices were fabricated on flexible substrates utilizing standard screen-printing techniques and afforded fully functional devices that were able to operate under ambient conditions. Since then the popularity of **PEDOT:PSS** has further increased, in particular due to its low-cost and availability as either aqueous dispersions or precast films. Consequently, the ion-to-electron conversion capabilities of **PEDOT:PSS**-based OECTs have been vastly improved over the last decade, with switching speeds for **PEDOT:PSS** nowadays reaching values for τ_{ON} and τ_{OFF} around 100 µs (for a channel w of 15 µm, l of 6 µm, and d of 80 nm).[79] High switching speeds are relevant for OECTs in biological sensing, as several physiological processes occur in the millisecond range, such as neuronal action potentials, thus requiring adequate devices for signal recording.[80] Additional investigations into the switching speeds of **PEDOT:PSS**-based OECTs revealed that the main factor limiting the switching speeds in such devices was the ionic circuit, i.e. the transport of ions into and out of the channel, thus leaving room for improvement in the coming years.[39]

Great strides in the optimization of **PEDOT:PSS**' g_m have also been made over the years, with the best performing device now reaching 4.0 mS.[39] An interesting finding in these results was that high g_m values could be preserved also after significant mechanical deformation, further highlighting the all-round benefits conferred by a **PEDOT:PSS** channel. An alternative strategy to improve **PEDOT:PSS**' performance can be achieved by the addition of an additive, such as ethylene glycol, during active layer casting. Here ethylene glycol's function is to fine-tune the morphology of the channel with respect to its ionic and electronic mobility. Studies have shown that upon augmenting the ethylene glycol content, film heterogeneity, domain purity, and **PEDOT**'s π–π aggregation increase.[81,82] These changes in turn had opposing effects on the ionic and electronic charge transport, whereby ionic conductivity suffered from the denser **PEDOT** rich domains, while electronic mobility significantly benefited. Ultimately, the best OECT performance was established at 5% ethylene glycol content, which struck the best balance between these opposing factors.[82] Despite the various attractive features of **PEDOT:PSS** highlighted above, one disadvantage is the acidic nature of its PSS, leading to corrosion in printheads and materials surrounding the active layer. A novel family of **PEDOT** derivatives was therefore devised in 2014 based on less acidic (trifluoromethylsulfonyl)sulfonylimide (TFSI) polyelectrolytes, with the anions shown in Figure 5.[83] TFSI was incorporated into polystyrene (PS) and polymethacrylate (PMA) backbones of different length, affording **PEDOT:PSTFSILi100**, **PEDOT:PSTFSIK20**, **PEDOT:PSTFSIK250**, and **PEDOT:PMATFSILi80**. OECT performance was subsequently evaluated. Here, devices utilizing the various styrenic counter anions, **PEDOT:PSTFSILi100**, **PEDOT:PSTFSIK20**, and **PEDOT:PSTFSIK250**, performed very well and were able to match the performance of state-of-the-art **PEDOT:PSS** devices in terms of both switching speeds and transconductance with τ_{OFF} values between 34 and 90 µs and g_m between 2.5 and 3.5 mS (for channels with a w of 100 µm, l of 10 µm, and d of 200 nm). **PEDOT:PMATFSILi80**-based devices on the other hand performed relatively poorly, as their g_m did not reach even half those of **PEDOT:PSS** devices. This was attributed in part to **PEDOT:PMATFSILi80**'s low hole conductivity, around 30 times lower than **PEDOT:PSS**' as well as its lower swelling ability, leading to reduced ion transport.

**ADVANCED
SCIENCE NEWS**
www.advancedsciencenews.com

**ADVANCED
FUNCTIONAL
MATERIALS**
www.afm-journal.de

Figure 6. Chemical structures of the various conjugated polyelectrolytes used as OECT channel materials.

While **PEDOT:PSS** as a channel material significantly advanced the performance of OECTs in terms of device g_m, switching speeds and stability, **PEDOT:PSS** still presents several drawbacks including its: i) highly complex structure, limiting its use as a model for polymer architecture–device performance investigations, ii) inability to be fully reduced to its charge neutral form, thereby incurring lower on–off ratios than could be achieved by alternative channel materials, and iii) limited volumetric capacitance, arising from the bulky nature of PSS severely reducing the "active" ratio of the material.[32,84] To tackle these limitations, the last 4 years have witnessed the development of a library of novel OECT materials, based on both conjugated polyelectrolytes (CPEs) and glycolated semiconducting polymers (GSPs).
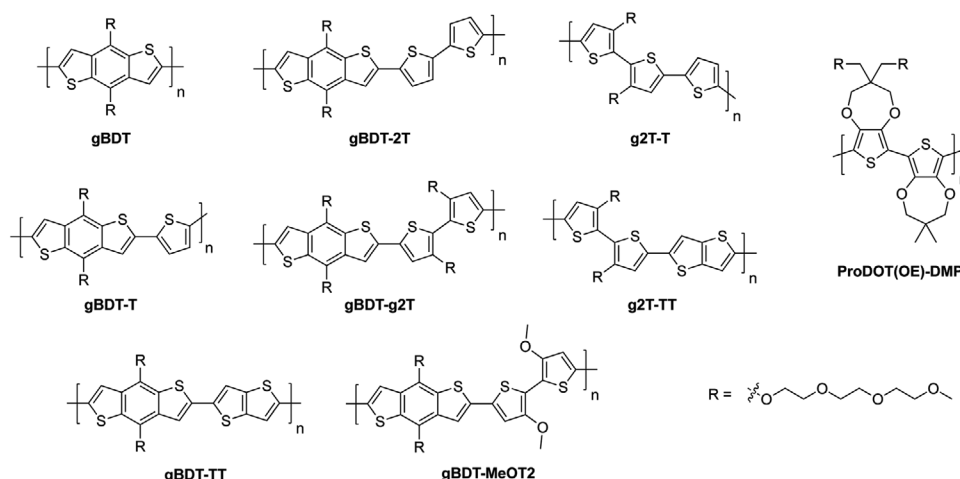
2014 witnessed the first report of a CPE for OECT applications, namely **PTHS**, which was based on a thiophene backbone and hexanesulfonate side chains, see **Figure 6**.[85] The design rationale behind **PTHS** was to combine the high hole mobility intrinsic to polythiophenes with the hydrophilic nature of sulfonates thereby ensuring efficient ion transport in and out of the channel as well as circumventing the need to include the inert polystyrene scaffold required for **PEDOT:PSS**.[86,87] Moreover, previous investigations into CPEs revealed **PTHS** to have the highest hole mobility in OFET devices amongst a series of polythiophene CPE derivatives.[88] The lack of any electron-donating oxygen substituents directly conjugated with the polythiophene backbone also shifted the HOMO of **PTHS** to a sufficiently low energy to prevent self-doping or doping in ambient conditions, allowing the OECTs to be operated in accumulation mode. Optimized devices gave a maximum g_m of 2.0 mS at a V_G of −0.8 V, on–off ratios of 700, and τ_{ON} of 0.4 ms (for a channel with a w of 250 µm, l of 5 µm, and d of 60 nm). The rather slow temporal response in devices was attributed to a relatively low ionic conductivity, which in turn could also rationalize the lower performance of **PTHS**-based OECTs compared to their **PEDOT:PSS** counterparts.

Poly(4-(2,3-dihydrothieno-(3,4-b)-(1,4)dioxin-2-yl-methoxy)-1-butanesulfonic acid, sodium salt) (**PEDOT-S**), shown in Figure 6, was first reported in 1998 and has a polymer backbone that closely resembles that of **PEDOT**.[89] The key difference between the two species lies in the additional sulfonate functionalized alkyl chain grafted onto the 3,4-ethylenedioxy bridge of each **PEDOT-S** repeat unit, conferring it with polyelectrolyte properties. Extensive evaluation of **PEDOT-S** as an OECT channel material was performed from 2015 onward, by fabricating devices based on either pristine **PEDOT-S** or in blends with other CPEs. **PEDOT-S** was originally chosen as a channel material due to its high electrical conductivity and high redox stability. These properties were reflected in the high g_m of 16.2 mS at a V_G of +0.2 V obtained in devices, which

then represented the highest g_m obtained in OECTs.[45] The relatively low on–off ratio obtained, 650, was comparable to that of **PTHS**, while switching speeds were significantly slower. A shortcoming of the devices was also their depletion mode of operation, thus **PEDOT-S** was blended with another CPE that operated in accumulation mode, sodium poly(2-(3-thienyl)ethoxy-4-butylsulfonate) (**PTEBS**), in ratios of 1:1, 2:3, and 1:2. The low fraction of **PEDOT-S** in the blends was chosen to avoid depletion type device characteristics. OECTs fabricated from the various **PEDOT-S:PTEBS** blends afforded slightly lower g_ms compared to neat **PEDOT-S** devices, with values between 9.0 and 12.0 mS. On–off ratios were similar to those of **PEDOT-S**; however, switching times were improved by a factor of 2–5 as a result of the rough fibrillar morphology, which enhanced ion transport. One key limitation of each of the **PEDOT-S**-based devices was their solubility in water hence the necessity to employ an ionic liquid, BMIMBF₄, as the electrolyte to allow for their operation. As a result, their application as sensing elements for biological applications that typically occur in aqueous solvents may be limited. The hydrophilic/hydrophobic character of **PEDOT-S**-based CPEs was later adjusted by counterion exchange with ammonium salts, specifically nonylammonium chloride ((Nonyl)NH₃Cl) and dioctylammonium chloride ((Oct)₂NH₂Cl) as these cations were found to impart processability in organic solvents while preventing CPE dissolution in water.[36] The resulting polymers, **PEDOT-S:(Nonyl)NH₃** and **PEDOT-S:(Oct)₂NH₂**, were prepared from **PEDOT-S** by addition of excess ammonium salts, whereby the equilibrium was further pushed toward the resulting ammonium CPEs by precipitation from an aqueous solvent. OECT performances of **PEDOT-S:(Nonyl)NH₃** and **PEDOT-S:(Oct)₂NH₂** were evaluated under aqueous conditions giving maximum g_ms of 7.0 and 11.0 mS, respectively. For **PEDOT-S:(Nonyl)NH₃**-based devices, severe hysteresis was observed in their transfer curves, indicating only limited reversibility of the ion injection/ejection process. This behavior was further complicated by the hybrid mode of operation and "overcharging" effect of **PEDOT-S:(Nonyl)NH₃** leading to a highly complex and oddly shaped transconductance curve. Interestingly, these features could not be observed in **PEDOT-S:(Oct)₂NH₂**-based OECTs, leading to speculation of the different morphologies of **PEDOT-S:(Nonyl)NH₃** and **PEDOT-S:(Oct)₂NH₂** to account for these differences. Stability measurements were also conducted and further supported the varying reversibility of the ion transport process in the two CPEs, with **PEDOT-S:(Nonyl) NH₃** retaining 71% of its initial electroactivity after 100 cycles and **PEDOT-S:(Oct)₂NH₂** not showing any signs of degradation after >10⁴ cycles.

Recently, OECT performance was increased by exploiting the synergies between the two previously developed strategies

**ADVANCED
SCIENCE NEWS**
www.advancedsciencenews.com

**ADVANCED
FUNCTIONAL
MATERIALS**
www.afm-journal.de

Figure 7. Chemical structures of the various p-type glycolated semiconducting polymers used as OECT channel materials.

(blending of two CPEs and cation substitution).[90] The starting point in these studies was **PTHS**, which was evaluated as the first channel material and achieved a g_m of 12.2 mS, an on–off ratio of 3.1×10^4, and τ_{ON} and τ_{OFF} of 428 ms and 62 ms, respectively (for a channel with a w of 1125 µm, l of 20 µm, and d of 133 nm). The next step involved fabricating devices with a 1:1 blend of **PTHS:PEDOT-S**. These had superior performance with a g_m of 13.7 mS, an on–off ratio of 8.8×10^4, and τ_{ON} and τ_{OFF} values of 91 and 16 ms (for a channel with a w of 1125 µm, l of 20 µm, and d of 102 nm), respectively. The final and crucial step in these investigations, involved replacement of **PEDOT-S** by **PEDOT-S:(Oct)$_2$NH$_2$** in the blends, yielding **PTHS:PEDOT-S:(Oct)2NH2**. **PTHS:PEDOT-S:(Oct)2NH2** displayed improved g_m of 15.3 mS and switching speeds of τ_{ON} and τ_{OFF} of 79 and 11 ms (for a channel with a w of 1125 µm, l of 20 µm, and d of 112 nm) compared to **PTHS:PEDOT-S**, while the on–off ratio of 4.4×10^4 was lower. Device stability also improved from 59% for **PTHS:PEDOT-S** to 88% for **PTHS:PEDOT-S:(Oct)$_2$NH$_2$** after 2×10^3 cycles; however, neither of these values matched the 90% retention of I_{SD} seen in the **PTHS** devices. Although strictly speaking, device performance was not improved with respect to each metric, overall this design strategy proved to be very successful considering its simplicity and potential applicability to future CPE systems.

3.3. GSPs

An exciting new class of materials in the domain of OECTs comprises semiconducting polymers with pendant ethylene glycol chains. In simple terms, in common with CPEs, the π-conjugated system of the GSP backbones is responsible for electronic charge transport, while the hydrophilic side chains are designed for efficient ion transport. Ample evidence in the literature however suggests that the positioning and length of oxygen bearing side chains also strongly impacts the optoelectronic and morphological properties of semiconducting polymers.[91–93] The first report on glycolated semiconducting polymers for OECT applications was published in 2016 and involved the synthesis of polymers containing either a glycolated benzodithiophene or bithiophene unit, see **Figure 7**.[32] These

monomers were chosen specifically, as both: i) allowed the first oxygen atom of their ethylene glycol chains to be directly grafted onto the polymer backbone, without the presence of any carbon spacers, thereby benefiting from its electron-donating nature and ii) afford highly planar polymer backbones, thereby replicating some of the advantageous molecular features presented by **PEDOT:PSS**. Homo- or copolymerization by Stille crosscoupling of the abovementioned moieties with either thiophene or bithiophene yielded five polymers: **gBDT**, **gBDT-T**, **gBDT-2T**, **gBDT-g2T**, and **g2T-T**. OECTs were subsequently fabricated for each polymer and revealed substantially inferior peak transconductances for those based on glycolated benzodithiophene compared to those based on glycolated bithiophene. The low performance of **gBDT**, **gBDT-T**, and **gBDT-2T** was attributed to their meager hole mobilities around 5×10^{-3} cm^2 V^{-1} s^{-1}, partially a consequence of their relatively large π-stacking distances of 3.7 Å. Furthermore, **gBDT**, **gBDT-T**, and **gBDT-2T** all featured relatively poor electrochemical properties, partially due to their relatively low-lying HOMOs around −4.85 eV, and demonstrated in their scarce electrochromic activity, which is indicative of the inherent difficulty to electrochemically dope the polymers. From a molecular point of view, these findings were partially linked to the limited ability of the glycolated benzodithiophene unit to afford highly planar backbone structures, compared to the glycolated bithiophene unit. In this aspect, the planarizing S—O interactions in the glycolated bithiophene moiety were particularly beneficial, affording dihedral angles around the central C—C bond close to 0°. A direct consequence of this molecular feature were the 0.4 eV higher HOMOs of **gBDT-g2T** and **g2T-T** as well as the appearance of a significantly more intense polaron absorption band during spectroelectrochemical measurements. Ultimately devices based on **gBDT-g2T** and **g2T-T** were able to achieve g_ms of 0.47 and 7.9 mS, respectively, whereby **g2T-T**'s tighter π-stacking distances and its preferential edge-on orientation on substrates were identified as the main causes for its higher hole mobilities hence performance. **g2T-T**'s transconductance was further enhanced by changing casting technique and optimizing device dimensions, culminating in a then unprecedented g_m of 21 mS with on–off ratios of 2.6×10^5. To unambiguously prove **g2T-T**'s superior g_m

compared to **PEDOT:PSS**-based devices, the g_ms of a set of ten devices for each material with varying channel geometries were fabricated, each confirming the above results.

In a follow-up study the performance and stability of polymers based on a glycolated benzodithiophene unit were further improved.[94] In that instance, glycolated benzodithiophene was copolymerized with thieno[3,2-b]thiophene (TT) and 3,3'-dimethoxy-2,2'-bithiophene, affording **gBDT-TT** and **gBDT-MeOT2**, respectively (shown in Figure 7). Compared to the **gBDT-2T** reference, both **gBDT-TT** and **gBDT-MeOT2** displayed higher HOMO energies of −4.70 and −4.31 eV, respectively, leading to lower turn-on voltages of the resulting OECTs. Ultimately, **gBDT-MeOT2**-based devices achieved not only the highest g_m of 1.82 mS but also stability, with on-currents stable for 300 cycles.

The newer material **g2T-TT** can be considered analogous to **g2T-T**, where 3,3'-bistriethyleneglycol-2,2'-bithiophene was retained as one of the repeat units and thiophene replaced by a more rigid TT moiety.[95] The effects of this substitution were negligible with respect to the optoelectronic properties of the material, as both the bandgap and HOMO–LUMO energy levels were virtually identical for **g2T-TT** and **g2T-T**. From a morphological perspective, incorporation of TT however resulted in shorter π–π stacking distances as confirmed by 2D grazing incidence X-ray scattering therefore suggesting a slightly more crystalline character of **g2T-TT**. The benefit of this feature was reflected in the augmented hole mobility of **g2T-TT** compared to that of **g2T-T**, with values of 0.95 and 0.28 cm^2 V^{-1} s^{-1}, respectively. Ultimately, this also resulted in the highest reported transconductance for OECTs, to date, with a g_m of 27 mS. Switching times for **g2T-TT** were also rapid, with τ_{ON} of 420 µs and τ_{OFF} of 43 µs (for a channel with a w of 100 µm and l of 10 µm), on–off ratios were in a similar regime of 10^5 compared to **g2T-T**.

Very recently, a new polymer backbone, **ProDOT(OE)-DMP** (shown in Figure 7), based on alternating an oligoethylene glycol functionalized ProDOT with an unfunctionalized ProDOT has been reported as an OECT channel material.[96] ProDOT was selected over 3,4-ethylenedioxythiophene (EDOT) as a monomer due the facile chemical modification of its propylene bridge, allowing for the incorporation of solubilizing chains, while retaining some of EDOT's highly electron rich nature. From a synthetic point of view **ProDOT(OE)-DMP** represented a first in the field of OECTs, due to its synthesis by direct(hetero)arylation polymerization (DHAP) rather than by the conventional Stille crosscoupling approach, which has been shown to leave residual tin in polymers even after end-capping, soxhlet, and additional purification steps.[57] In the context of in vivo applications of OECTs this is a particularly attractive synthetic feature as DHAP foregoes the need of any organotin intermediates, which are known to be highly toxic to organisms and DHAP has been shown to leave less residual metal in polymers than other ponlymerization methods.[97,98] Ultimately, OECTs based on **ProDOT(OE)-DMP** afforded on–off ratios in excess of 10^5, similar to those of the 3,3'-bistriethyleneglycol-2,2'-bithiophene-based polymers and higher than those of current CPEs. However, **ProDOT(OE)-DMP**'s maximum g_m of 0.62 mS is relatively low compared to **g2T-TT**. This was predominantly due to **ProDOT(OE)-DMP**'s 15-fold lower hole mobility, likely arising from its twisted seven membered rings bearing neopentyl linkages on the ProDOT units, reducing

long range order in polymer films. Notably, this is also the first example of a glycolated OECT material to be designed around the backbone's capacitive behavior, high electrochromic contrast, and high electrochemical stability, rather than from modification of a typical OFET or OPV repeat unit design.

A summary of the molecular characteristics of the various channel materials employed, including the number average molecular weight (M_n), dispersity ($Đ$), degree of polymerization (X_n), and analytical technique employed is given in **Table 1**. The molecular weight of **PPy** and **PANI** cannot be determined

Table 1. Summary of the molecular characteristics of the various channel materials employed, including the number average molecular weight (M_n), dispersity ($Đ$), degree of polymerization (X_n) and analytical technique employed.

Channel material	M_n [kDa]	$Đ$	X_n	Analytical technique[a]
PTHS[85]	42.0	1.09	82	GPC (THF)
PTHS[90]	18.1[b]	1.14[b]	74[b]	GPC (THF)[b]
	18.5[b]	1.02[b]	75[b]	MALDI-TOF MS[b]
PEDOT-S[45]	–	–	–	–
PEDOT-S[36]	–[c]	–[c]	–[c]	–[c]
PEDOT-S[90,99]	1.7	3.2	5	GPC (–)
PTEBS[45]	–	–	–	–
PEDOT-S:(Nonyl)NH3[36]	–	–	–	–
PEDOT-S:(Oct)2NH2[36]	–	–	–	–
PEDOT-S:(Oct)2NH2[90]	–	–	–	–
gBDT[32]	4.2	1.5	8	GPC (CB)
gBDT-T[32]	–	–	–	–
gBDT-2T[32]	–	–	–	–
gBDT-g2T[32]	22.1	1.9	22	GPC (DMF)
g2T-T[32]	62.5	1.6	109	GPC (DMF)
gBDT-TT[94]	–	–	–	–
gBDT-MeOT2[94]	–[d]	–[d]	–[d]	MALDI-TOF MS[d]
g2T-TT[95]	10.0	2.0	16	GPC (CHCl$_3$:DMF, 5:1)
ProDOT(OE)-DMP[96]	22.5	2.0	31	GPC (CHCl$_3$)
p(gNDI-gT2)[100]	–[d]	–[d]	–[d]	–[d]
p(gNDI-T2)[100]	–	–	–	–
P-0[101]	18.0	1.8	19	GPC (CB)
P-10[101]	18.4	1.8	19	GPC (CB)
P-25[101]	15.3	1.8	15	GPC (CB)
P-50[101]	19.0	1.6	19	GPC (CB)
P-75[101]	16.7	1.4	15	GPC (CB)
P-90[101]	7.8	1.6	7	GPC (CB)
P-100[101]	7.2	1.3	7	GPC (CB)
BBL[102]	–	–	–	–

[a]Analytical measurement performed either by gel permeation chromatography (GPC) with instrument calibrated against polystyrene standards or matrix assisted laser desorption ionization spectroscopy-time of flight mass spectrometry (MALDI-TOF MS). The various GPC solvents employed are tetrahydrofuran (THF), chlorobenzene (CB), dimethylformamide (DMF), chloroform (CHCl$_3$). [b]Molecular weight characterization was performed on the precursor polymer P3BrHT; [c]Structures with up to 16 repeat units detected by matrix assisted laser desorption ionization spectroscopy (MALDI); [d]Structures with up to seven repeat units detected by MALDI.

via conventional methods as the polymers are prepared electrochemically and are insoluble films on electrodes. Additionally, dispersions of **PEDOT**, such as **PEDOT:PSS**, are typically not characterized in terms of molecular weight as they are insoluble doped oligomers in a soluble polymer matrix. It can be seen from Table 1 that there is a large range of molecular weights from the materials studied and the role of molecular weight in OECT polymers is currently unclear.

4. n-Type OECT Channel Materials

While each of the previously discussed materials for OECTs has been based on hole transporting semiconducting or conducting polymers, we now discuss n-type OECT channel materials, which did not appear until 2016.[100] The development of n-type materials is however crucial, especially for the application of OECTs as biological sensing elements, such as for cation sensing or metabolite sensing via enzyme conjugation, which generally operates by an electron-transfer rather than hole-transfer process.[33] Furthermore, n-type channel materials are also important for the realization of complementary logic circuits, thereby expanding the capabilities of OECTs.

p(gNDI-gT2) is based on an alternating naphthalene-1,4,5,8-tetracarboxylic diimide (NDI) and bithiophene (T2) polymer backbone, similar to the well-known polymer **N2200,** with each of the two building blocks functionalized with ethylene glycol chains, shown in **Figure 8**.[100] An analogue of **p(gNDI-gT2)** in which the glycol chains have been omitted from the bithiophene moiety was also synthesized, **p(gNDI-T2)**; however, compared to **p(gNDI-gT2)** did not exhibit ambipolar charge transport properties due to its 0.7 eV lower lying HOMO. Recently, a series of NDI-T2-based polymers with slightly modified and elongated ethylene glycol chains compared to **p(gNDI-T2)** was reported.[101] In this study the linear ethylene glycol side chains were gradually replaced by branched alkyl ones, affording seven random copolymers: **P100**, **P90**, **P75**, **P50**, **P25**, **P10,** and **P0**, with glycol chain percentages of 100, 90, 75, 50, 25, 10, and 0, respectively. For the polymers with a glycol side chain percentage <75%, no functional n-type OECT behavior was observed due to the inability of these polymers to charge volumetrically. These findings were corroborated both by quartz crystal microbalance with dissipation monitoring and CV, indicating poor swelling behavior and ion uptake. Alternatively, fully

functional OECTs were fabricated for polymers incorporating higher glycol side chain fractions (**P75**, **P90**, and **P100**), all showing similar performances and reaching a maximum g_m of 1.1 μS. Nevertheless, neither of these could compete with **p(gNDI-gT2)**-based devices, where peak g_m values of 21.7 μS and 13.4 μS and on–off ratios of 3.2×10^3 and 2.0×10^2 were obtained for n-type and p-type operation, respectively. Although these results are encouraging, significant research efforts are still required to improve the n-type OECT performance of GSPs compared to their already excellent p-type analogues. In particular, their low electron mobilities around 10^{-5} cm^2 V^{-1} s^{-1} must be improved substantially to minimize this performance gap. It is possible that the localized nature of the charge carriers in NDI-T2-based polymers, which contributes to their low solid-state conductivities when doped, may be limiting their OECT performance.[103] In this aspect, a departure from the current donor–acceptor polymer structures toward all-acceptor ones may offer the desired outcomes. The potential benefits of such an approach have already been demonstrated in the literature. For example, when taking the donor–acceptor polymer **N2200** as reference (which can be considered as structurally similar to **p(gNDI-gT2)**), n-type doping performed with a range of dopants afforded a poor maximum solid state conductance (σ_{max}) ranging between 3.0×10^{-3} and 8.0×10^{-3} S cm^{-1}, despite achieving a near quantitative doping reaction.[104,105] Substitution of the electron-donating bithiophene comonomer in **N2200** with more electron-withdrawing ethynylene and diethynylbenzothiadiazole units, on the other hand, afforded polymers with improved σ_{max}, spanning between 0.07 and 0.45 S cm^{-1}.[105] UV–vis spectroscopy was employed to study the origin of this behavior, as the P1 transition energy and the extent of neutral polymer quenching by each charge can be used as a measure of the polaron delocalization length. For the reference **N2200** polymer, a polaron delocalization length of 1.25 nm was estimated. On the other hand, for the ethynylene and diethynylbenzothiadiazole based polymers, significantly longer polaron delocalization lengths between 3.00 and 4.50 nm were obtained, thus highlighting their more delocalized nature, which in turn was attributed to their better charge transport ability. One of the most interesting points to note in these studies is that the polymers incorporating the ethynylene and diethynylbenzothiadiazole moieties had OFET electron mobilities approximately one order of magnitude lower than that of the **N2200** reference, indicating that the design rules for high performance OFET
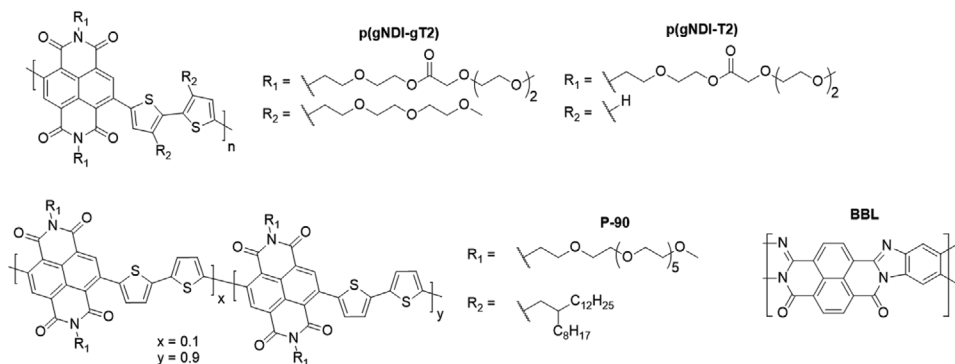
Figure 8. Chemical structures of the various n-type semiconducting polymers used as OECT channel materials.

**ADVANCED
SCIENCE NEWS**
www.advancedsciencenews.com
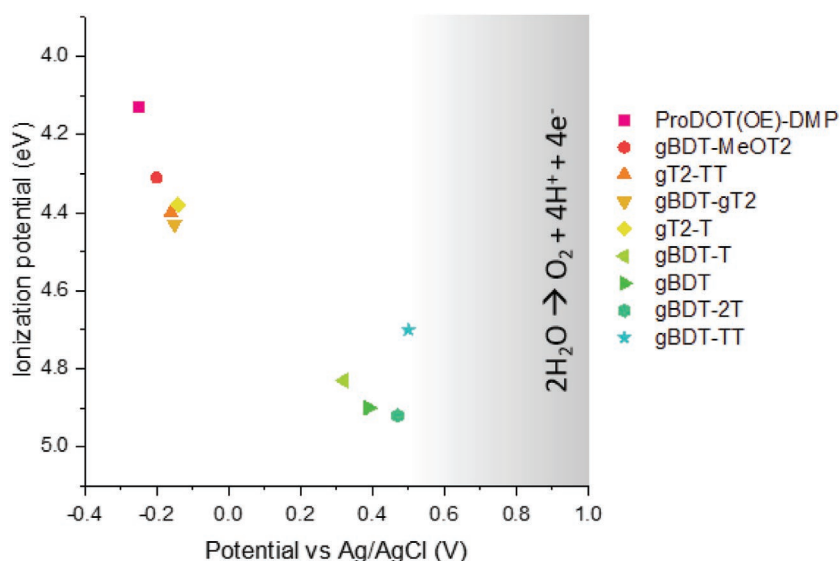
**ADVANCED
FUNCTIONAL
MATERIALS**
www.afm-journal.de

applications do not necessarily hold true for n-type doping applications. Similar conclusions were also found when comparing **N2200** with the ladder-type polymer, poly(benzimidazobenzophenanthroline) (**BBL**).[103] In this instance n-type doping of **N2200** once again afforded a σ_{max} around 10^{-3} S cm^{-1}, whilst **BBL**'s fully n-type and rigid polymer backbone was shown to boost the polaron delocalization length over three rather than a single repeat unit, which was subsequently used as justification for **BBL**'s almost 500-fold larger σ_{max}. Because **BBL**'s comparatively high σ_{max} was envisaged to potentially benefit OECT performance, n-type OECTs employing **BBL** as a channel material were recently fabricated.[102] The resulting devices achieved a g_m and on–off values of 9.7 mS and 6000, respectively. However, when taking into consideration device geometry, the performance of **BBL** only resulted in an ≈2.5 times higher transconductance compared to **p(gNDI-gT2)**, thus indicating that σ_{max} alone may also not be an ideal parameter for predicting a material's OECT performance. Additionally, one drawback of **BBL**-based OECTs was their very slow switching speeds with τ_{ON} of 0.9 s and τ_{OFF} of 0.2 s (for a channel with a w of 39 mm, l of 20 μm, and d of 180 nm), indicating ion migration into the polymer film as the limiting element in device performance. The inclusion of hydrophilic side chains into the polymer structure could potentially provide a straightforward solution toward this issue, as it is known that ions have higher mobilities through side chain rich regions of films. However, care must be taken to avoid disrupting the conductive polymer backbone. Ultimately, the OECT performance obtained from both NDI-T2 and all-acceptor based polymers are still lagging those of their p-type analogues thus highlighting the necessity to develop better performing materials. The molecular weight information of the n-type polymers discussed is listed in Table 1.

Figure 9. Ionization potentials and onset of oxidation of various p-type OECT channel materials. The gray shaded region indicates the onset of water oxidation at 25 °C and pH = 7, relative to a Ag/AgCl reference electrode. All ionization potentials are given relative to vacuum and potentials relative to a Ag/AgCl reference electrode based on a potential of 4.67 eV relative to vacuum; exact values against Fc/Fc$^+$ may vary slightly. The onset of oxidation for the p-type OECT channel materials have been measured employing water as the solvent and NaCl/H_2O as the electrolyte.

5. General Design Principles

5.1. p-Type Design

Following the initial use of **PPy** and **PANI**, the majority of high performance OECT active materials to date can be divided into two general classes: those based on **PEDOT** and those based on known OFET polymer structures. This is unsurprising as doped **PEDOT** and **PEDOT** derivatives can have high solid-state electrical conductivities and a large amount of research has been performed developing design rules for transistor materials. Despite the limited range of structures previously explored, general design features for future materials can be outlined.

From all of the high performing materials it can be seen that backbone planarity is of utmost importance. Planar backbones can afford tight π-stacking, depending on additional factors

including side chains, which benefits hole and electron transport within the film. This was previously discussed, with **g2T-TT** showing closer π-stacking and a higher transconductance compared to **g2T-T**. However, care must be taken as it has been shown with both **PEDOT:PSS** and alkyl functionalized polymers that increased order in a film can reduce electrochemical switching speeds due to slow ion transport through ordered domains.[82]

Another important consideration is the ionization potential (*IP*) of the polymer, which is primarily dictated by the HOMO of the polymer film. Foremost, the *IP* must be sufficiently small to allow doping of the polymer within the electrochemical potential window of water (H_2O/O_2 oxidation at pH 7 of 5.3 eV and H^+/H_2 reduction at pH 7 of 4.05 eV).[106,107] Polymers with small *IPs* also tend to be more stable to repeated electrochemical cycling, see **Figure 9**. However, an excessively shallow *IP* will result in the polymer being doped, and hence conducting, under ambient conditions, potentially leading to depletion mode behavior, which may or may not be reversible depending on the nature of the polymer and generally results in lower on/off ratios. 3-alkoxy and 3,4-dialkoxy substituents on thiophenes have been found to be effective at reducing the *IP* (raising the HOMO) and increasing the electrochemical stability of polymers under OECT operation. This improved stability can come from either lowering the *IP* so that other functionalities do not degrade, such as with **gBDT-2T** and **gBDT-MeOT2**,[94] or by blocking positions on the polymer chain where degradation/crosslinking could occur, such as is the case with **ProDOT(OE)-DMP** and other dioxythiophene polymers.[96] Fine tuning of the *IP* by changing the relative number of these units and the steric bulk/twisting of the alkyl (and sometimes aryl) groups has been extensively studied in the organic

**ADVANCED
SCIENCE NEWS**
www.advancedsciencenews.com

**ADVANCED
FUNCTIONAL
MATERIALS**
www.afm-journal.de

electronics, electrochromic[108–111] and computational literature[112–114] and will not be discussed in detail here.

5.2. n-Type Semiconducting Polymer Backbone Design

With the exception of **BBL**, only NDI based systems have so far been studied for n-type OECTs, thus limiting the design rules that can be extrapolated from the above discussion. Nonetheless, it can be concluded that the primary factor limiting n-type material OECT performance so far has been their low electron mobility and will thus have to be the main parameter of focus in future studies. Considering that **N2200**, which is structurally similar to the NDI-T2 based OECT channel materials, displays a good electron mobility in excess of 0.8 cm^2 V^{-1} s^{-1} in OFETs, the low mobilities of NDI-T2 based channel materials is somewhat surprising.[115] Although the origin of this discrepancy between electron mobility in OFETs and OECTs has so far not been elucidated, a potential explanation may be due to the use of an aqueous electrolyte in OECTs. Unlike in OFETs that can be operated under inert atmosphere conditions, the presence of water in OECTs requires the electron affinity (*EA*) of the channel material to be at least lower than −4.05 eV relative to vacuum to fall within the solvent's electrochemical stability window. As the *EA*s of both **p(gNDI-gT2)** and **BBL** lie close to −4.0 eV, neither of these polymers may have a sufficiently low *EA* to fully prevent any undesirable proton reduction and simultaneous dedoping of the channel material, which in turn could explain their low mobilities in OECTs.

An alternative explanation for the low electron mobility observed in n-type channel materials compared to their p-type counterparts could also be due to polaron charge balancing occurring by the influx of Na$^+$ ions rather than Cl$^-$ ones. As demonstrated in the literature, the influx of Na$^+$ ions into p-type OECT channel materials has been shown to be accompanied by the concomitant influx of two to four water molecules per cation, whilst the influx of Cl$^-$ ones by 10 per anion.[116,117] Consequently, it is to be expected that the ionic charge on Na$^+$ ions will not be screened as efficiently as those on Cl$^-$ ones. A likely ramification of this is stronger electrostatic interactions between the electron polaron on the polymer backbone and the influx of cations, essentially leading to a charge pinning effect and reducing the electron mobility in n-type channel materials.

5.3. Side Chain Designs

Currently, the highest reported transconductance values and on/off ratios have been obtained from materials utilizing oligoether side chains and these are currently the side chain of choice for new OECT materials. When directly grafted onto the polymer backbone, the alkyl-aryl-ether linkage simultaneously provides electron donation, lowering the *IP* and stabilizing the oxidized (polaron or bipolaron) states, and leads to favorable noncovalent S—O interactions between rings, potentially resulting in more planar backbones. Moreover, the widespread commercial availability and low cost of ethylene glycol chains with varying chain lengths and functionalities further add to their attractiveness.

However, the optimal length of these glycol side chains has yet to be studied, with all current p-type GSPs using triethylene glycol monomethyl chains, selected to balance solubility with backbone packing. Changing the length of this chain and experimenting with branching points could be valuable for next generation materials with higher transconductances and/or improved processability. It is timely for this to now be investigated, as side chain engineering has been extensively studied for OFET and OPV discrete molecules and polymers and, to a lesser extent, for electrochromic polymers. The random or systematic incorporation of alkyl side chains into glycolated polymers, such as was carried out with **N2200** derivatives, could also prove fruitful. Asymmetric alkylation of DPP with an alkyl and a glycol chain was recently reported for discrete molecule OFETs and could potentially also be a valuable alternative for OECT materials.[118] An alternative option is implementation of different hydrophilic side chains. One example of this involved a polymer based on a DPP backbone, this time functionalized with lysine side chains, that was used for neural cell growth.[119] Unfortunately, there was no report of OECT performance, most likely as the DPP backbone has an excessively low *IP* such that efficient doping in an aqueous environment is not possible. Carboxylic acid side chains have also been shown to allow for stable redox switching of polymers for >10^5 cycles in aqueous electrolytes and even using blood as the electrolyte.[78,120] However, these materials have yet to be studies in OECTs.

6. Conclusions and Outlook

Since its inception in 1986, the organic electrochemical transistor has become a well-established device in the bioelectronics community, in particular due to its excellent transducing properties, relatively simple device structure, and applicability for signal recording in biological systems.[47] Compared to dielectric and electrolyte-gated organic field effect transistors, the operating mechanism of OECTs differs significantly as doping of the semiconductor channel is not restricted to its interface but occurs throughout the bulk of the material. Because of this requirement for efficient operation, organic semiconductors capable of conducting both ionic and electronic charge carriers have emerged as successful channel materials. Great strides have been made over the past 15 years in the development of increasingly better performing channel materials, especially with the introduction of **PEDOT:PSS** as a channel material. Here, the high hole transporting ability, chemical stability, and in particular the widespread commercial availability of **PEDOT:PSS** have cemented its status as the golden standard. Despite these attractive properties, its highly complex structure has severely hampered its use as a model for polymer structure–property relationship investigations, thus suggesting its use arises predominantly out of convenience rather than out of performance alone. To tackle this drawback, the past 5 years have witnessed a rapid increase in the number of novel OECT materials, in particular p-type ones, based on either conjugated polyelectrolytes or glycolated semiconducting polymers. Both material classes have shown tremendous success as channel materials and have repeatedly outperformed **PEDOT:PSS**-based references, which is attributed to their higher reported

volumetric capacitances, while providing the field with numerous insights into the molecular design of channel materials for efficient OECT operation. The departure from the **PEDOT:PSS** backbone has also enabled the evolution of n-type channel materials; however, their performance has yet to consistently match their p-type counterparts. While further development of p-type materials will be of value to the field, there is a greater need and room for growth in n-type semiconductors, especially due to their relevance in biological sensing including both metabolite and cation recognition.

Recently, advances in the synthesis of the channel materials have also been achieved. In this context, a shift from conventional Stille polymerization conditions toward direct arylation polymerizations may offer simpler, faster, and more atom economical synthetic routes toward future channel materials. Despite this synthetic progress, a frequently encountered issue for both p-type and n-type channel materials still lies in their limited solubility in common organic solvents, which can not only limit their molecular weight and processability but also complicate their molecular weight determination. A potential solution to forego this problem in the future may be through the introduction of longer or branched ethylene glycol side chains. These may however complicate the purification of the resulting synthetic intermediates by conventional techniques employed in the field of organic electronics, especially due to their expected increased solubility in aqueous media and waxy nature. This in turn could further convolute the synthesis of the OECT channel materials, by creating stoichiometric imbalances during the polymerization step, which according to the Carothers equation would result in low molecular weight polymers.

Lastly, we also expect advances to be made in device fabrication methods and architecture to further boost OECT performance. This follows from the discussion that drop-cast active layers have, for example, been demonstrated to achieve g_ms almost twice as high as their spin-cast counterparts, while employing identical channel dimensions.[32] The choice of electrolyte may also offer further performance improvements. Although most publications in the field employ a 0.1 M sodium chloride solution as the electrolyte of choice, others have also been explored.[36] In this context it is nontrivial to note that different electrolyte anions have shown to not only modulate the maximum doping level achieved in polymers but also transport properties in OECTs.

Overall, the understanding and performance of OECTs have been notably improved in the past 10 years, nonetheless we expect that in the coming years advances in both material developments and device fabrication will further push the frontiers of the field.

Conflict of Interest

The authors declare no conflict of interest.

[1] M. Berggren, A. Richter-Dahlfors, *Adv. Mater.* **2007**, *19*, 3201.
[2] J. Rivnay, R. M. Owens, G. G. Malliaras, *Chem. Mater.* **2014**, *26*, 679.
[3] B. C. Albensi, in *Encyclopedia of Basic Epilepsy Research* (Ed: P. A. Schwartzkroin), Academic Press, Oxford **2009**, p. 1426.
[4] A. L. Kip, D. U. Jeffrey, Y. Junyan, C. M. David, R. K. Daryl, *J. Neural Eng.* **2006**, *3*, 59.
[5] M. Asplund, E. Thaning, J. Lundberg, A. C. Sandberg-Nordqvist, B. Kostyszyn, O. Inganäs, H. v. Holst, *Biomed. Mater.* **2009**, *4*, 045009.
[6] D. Khodagholy, T. Doublet, P. Quilichini, M. Gurfinkel, P. Leleux, A. Ghestem, E. Ismailova, T. Hervé, S. Sanaur, C. Bernard, G. G. Malliaras, *Nat. Commun.* **2013**, *4*, 1575.
[7] K. W. Johnson, J. J. Mastrototaro, D. C. Howey, R. L. Brunelle, P. L. Burden-Brady, N. A. Bryan, C. C. Andrew, H. M. Rowe, D. J. Allen, B. W. Noffke, W. C. McMahan, R. J. Morff, D. Lipson, R. S. Nevin, *Biosens. Bioelectron.* **1992**, *7*, 709.
[8] H. Tang, F. Yan, P. Lin, J. Xu, H. L. W. Chan, *Adv. Funct. Mater.* **2011**, *21*, 2264.
[9] A.-M. Pappa, V. F. Curto, M. Braendlein, X. Strakosas, M. J. Donahue, M. Fiocchi, G. G. Malliaras, R. M. Owens, *Adv. Healthcare Mater.* **2016**, *5*, 2295.
[10] G. Horowitz, *Adv. Mater.* **1998**, *10*, 365.
[11] H. Sirringhaus, *Adv. Mater.* **2005**, *17*, 2411.
[12] J. Mei, Y. Diao, A. L. Appleton, L. Fang, Z. Bao, *J. Am. Chem. Soc.* **2013**, *135*, 6724.
[13] S. Allard, M. Forster, B. Souharce, H. Thiem, U. Scherf, *Angew. Chem., Int. Ed.* **2008**, *47*, 4070.
[14] W. Wu, Y. Liu, D. Zhu, *Chem. Soc. Rev.* **2010**, *39*, 1489.
[15] W. Brütting, S. Berleb, A. G. Mückl, *Org. Electron.* **2001**, *2*, 1.
[16] B. W. D'Andrade, S. R. Forrest, *Adv. Mater.* **2004**, *16*, 1585.
[17] B. Geffroy, P. le Roy, C. Prat, *Polym. Int.* **2006**, *55*, 572.
[18] C. M. Amb, A. L. Dyer, J. R. Reynolds, *Chem. Mater.* **2011**, *23*, 397.
[19] M. E. Abdelhamid, A. P. O'Mullane, G. A. Snook, *RSC Adv.* **2015**, *5*, 11611.
[20] B. Kippelen, J.-L. Brédas, *Energy Environ. Sci.* **2009**, *2*, 251.
[21] K. A. Mazzio, C. K. Luscombe, *Chem. Soc. Rev.* **2015**, *44*, 78.
[22] N. Gasparini, A. Wadsworth, M. Moser, D. Baran, I. McCulloch, C. J. Brabec, *Adv. Energy Mater.* **2018**, *8*, 1703298.
[23] A. Wadsworth, M. Moser, A. Marks, M. S. Little, N. Gasparini, C. J. Brabec, D. Baran, I. McCulloch, *Chem. Soc. Rev.* **2018**, https://doi.org/10.1039/c7cs00892a.
[24] E. Stavrinidou, P. Leleux, H. Rajaona, D. Khodagholy, J. Rivnay, M. Lindau, S. Sanaur, G. G. Malliaras, *Adv. Mater.* **2013**, *25*, 4488.
[25] D. T. Simon, E. O. Gabrielsson, K. Tybrandt, M. Berggren, *Chem. Rev.* **2016**, *116*, 13009.
[26] S. Inal, J. Rivnay, A.-O. Suiu, G. G. Malliaras, I. McCulloch, *Acc. Chem. Res.* **2018**, *51*, 1368.
[27] S. Stříteský, A. Marková, J. Vítecek, E. Šafaříková, M. Hrabal, L. Kubác, L. Kubala, M. Weiter, M. Vala, *J. Biomed. Mater. Res., Part A* **2018**, *106*, 1121.
[28] R. Mannerbro, M. Ranlöf, N. Robinson, R. Forchheimer, *Synth. Met.* **2008**, *158*, 556.

**ADVANCED
SCIENCE NEWS**
www.advancedsciencenews.com

**ADVANCED
FUNCTIONAL
MATERIALS**
www.afm-journal.de

[29] J. Y. Wong, R. Langer, D. E. Ingber, *Proc. Natl. Acad. Sci. USA* **1994**, *91*, 3201.

[30] D. Khodagholy, T. Doublet, M. Gurfinkel, P. Quilichini, E. Ismailova, P. Leleux, T. Herve, S. Sanaur, C. Bernard, G. G. Malliaras, *Adv. Mater.* **2011**, *23*, H268.

[31] T. Hanawa, S. Kuwabata, H. Hashimoto, H. Yoneyama, *Synth. Met.* **1989**, *30*, 173.

[32] C. B. Nielsen, A. Giovannitti, D.-T. Sbircea, E. Bandiello, M. R. Niazi, D. A. Hanifi, M. Sessolo, A. Amassian, G. G. Malliaras, J. Rivnay, I. McCulloch, *J. Am. Chem. Soc.* **2016**, *138*, 10252.

[33] A. M. Pappa, D. Ohayon, A. Giovannitti, I. P. Maria, A. Savva, I. Uguz, J. Rivnay, I. McCulloch, R. M. Owens, S. Inal, *Sci. Adv.* **2018**, *4*, eaat0911.

[34] P. Lin, F. Yan, *Adv. Mater.* **2012**, *24*, 34.

[35] X. Strakosas, M. Bongo, R. M. Owens, *J. Appl. Polym. Sci.* **2015**, *132*, n/a.

[36] E. Zeglio, J. Eriksson, R. Gabrielsson, N. Solin, O. Inganäs, *Adv. Mater.* **2017**, *29*, 1605787.

[37] D. T. Duong, Y. Tuchman, P. Chakthranont, P. Cavassin, R. Colucci, T. F. Jaramillo, A. Salleo, G. C. Faria, *Adv. Electron. Mater.* **2018**, *4*, 1800090.

[38] C. Pitsalidis, A.-M. Pappa, M. Porel, C. M. Artim, G. C. Faria, D. D. Duong, C. A. Alabi, S. Daniel, A. Salleo, R. M. Owens, *Adv. Mater.* **2018**, *30*, 1803130.

[39] D. Khodagholy, J. Rivnay, M. Sessolo, M. Gurfinkel, P. Leleux, L. H. Jimison, E. Stavrinidou, T. Herve, S. Sanaur, R. M. Owens, G. G. Malliaras, *Nat. Commun.* **2013**, *4*, 2133.

[40] D. A. Bernards, G. G. Malliaras, *Adv. Funct. Mater.* **2007**, *17*, 3538.

[41] F. Cicoira, M. Sessolo, O. Yaghmazadeh, J. A. DeFranco, S. Y. Yang, G. G. Malliaras, *Adv. Mater.* **2010**, *22*, 1012.

[42] P. C. Hütter, T. Rothländer, A. Haase, G. Trimmel, B. Stadlober, *Appl. Phys. Lett.* **2013**, *103*, 043308.

[43] G. Tarabella, C. Santato, S. Y. Yang, S. Iannotta, G. G. Malliaras, F. Cicoira, *Appl. Phys. Lett.* **2010**, *97*, 123304.

[44] S. E. Doris, A. Pierre, R. A. Street, *Adv. Mater.* **2018**, *30*, 1706757.

[45] E. Zeglio, M. Vagin, C. Musumeci, F. N. Ajjan, R. Gabrielsson, X. T. Trinh, N. T. Son, A. Maziz, N. Solin, O. Inganäs, *Chem. Mater.* **2015**, *27*, 6385.

[46] W. Kaim, J. Fiedler, *Chem. Soc. Rev.* **2009**, *38*, 3373.

[47] H. S. White, G. P. Kittlesen, M. S. Wrighton, *J. Am. Chem. Soc.* **1984**, *106*, 5375.

[48] E. W. Paul, A. J. Ricco, M. S. Wrighton, *J. Phys. Chem.* **1985**, *89*, 1441.

[49] S. Tanaka, T. Iso, *J. Chem. Soc., Chem. Commun.* **1994**, *0*, 1071.

[50] N. Wang, A. Kähkönen, P. Damlin, T. Ääritalo, J. Kankare, C. Kvarnström, *Electrochim. Acta* **2015**, *154*, 361.

[51] S.-C. Huang, C.-Y. Lin, *Chem. Commun.* **2015**, *51*, 519.

[52] J. Xia, N. Masaki, K. Jiang, S. Yanagida, *J. Mater. Chem.* **2007**, *17*, 2845.

[53] X. Cui, V. A. Lee, Y. Raphael, J. A. Wiler, J. F. Hetke, D. J. Anderson, D. C. Martin, *J. Biomed. Mater. Res.* **2001**, *56*, 261.

[54] S.-C. Luo, J. Sekine, B. Zhu, H. Zhao, A. Nakao, H.-h. Yu, *ACS Nano* **2012**, *6*, 3018.

[55] S. P. Ponnappa, S. Arumugam, H. J. Spratt, S. Manzhos, A. P. O'Mullane, G. A. Ayoko, P. Sonar, *J. Mater. Res.* **2017**, *32*, 810.

[56] J. Wang, G. Cai, X. Zhu, X. Zhou, *J. Appl. Polym. Sci.* **2012**, *124*, 109.

[57] C. K. Lo, B. R. Gautam, P. Selter, Z. Zheng, S. D. Oosterhout, I. Constantinou, R. Knitsch, R. M. W. Wolfe, X. Yi, J.-L. Brédas, F. So, M. F. Toney, V. Coropceanu, M. R. Hansen, K. Gundogdu, J. R. Reynolds, *Chem. Mater.* **2018**, *30*, 2995.

[58] M. Nishizawa, T. Matsue, I. Uchida, *Anal. Chem.* **1992**, *64*, 2642.

[59] C. O. Baker, X. Huang, W. Nelson, R. B. Kaner, *Chem. Soc. Rev.* **2017**, *46*, 1510.

[60] D. Kumar, R. C. Sharma, *Eur. Polym. J.* **1998**, *34*, 1053.

[61] A. G. MacDiarmid, *Synth. Met.* **1997**, *84*, 27.

[62] G. Williams, H. N. McMurray, *Electrochem. Solid-State Lett.* **2005**, *8*, B42.

[63] P. N. Bartlett, P. R. Birkin, *Anal. Chem.* **1993**, *65*, 1118.

[64] P. N. Bartlett, *Analyst* **1998**, *123*, 387.

[65] S. K. An. Elschner, W. Lövenich, U. Merker, K. Reuter, *PEDOT: Principles and Applications of an Intrinsically Conducting Polymer*, CRC Press, Boca Raton, FL **2011**.

[66] Q. Pei, G. Zuccarello, M. Ahlskog, O. Inganäs, *Polymer* **1994**, *35*, 1347.

[67] J. C. Gustafsson, B. Liedberg, O. Inganäs, *Solid State Ionics* **1994**, *69*, 145.

[68] O. Bubnova, Z. U. Khan, A. Malti, S. Braun, M. Fahlman, M. Berggren, X. Crispin, *Nat. Mater.* **2011**, *10*, 429.

[69] D. Alemu, H.-Y. Wei, K.-C. Ho, C.-W. Chu, *Energy Environ. Sci.* **2012**, *5*, 9662.

[70] F. Jonas, L. Schrader, *Synth. Met.* **1991**, *41*, 831.

[71] G. Heywang, F. Jonas, *Adv. Mater.* **1992**, *4*, 116.

[72] F. Zhang, M. Johansson, M. R. Andersson, J. C. Hummelen, O. Inganäs, *Adv. Mater.* **2002**, *14*, 662.

[73] D. Nilsson, M. Chen, T. Kugler, T. Remonen, M. Armgarth, M. Berggren, *Adv. Mater.* **2002**, *14*, 51.

[74] M. De Keersmaecker, A. W. Lang, A. M. Österholm, J. R. Reynolds, *ACS Appl. Mater. Interfaces* **2018**, *10*, 31568.

[75] A. M. Österholm, D. E. Shen, A. L. Dyer, J. R. Reynolds, *ACS Appl. Mater. Interfaces* **2013**, *5*, 13432.

[76] A. M. Österholm, J. F. Ponder, J. A. Kerszulis, J. R. Reynolds, *ACS Appl. Mater. Interfaces* **2016**, *8*, 13492.

[77] T. Cheng, Y.-Z. Zhang, J.-D. Zhang, W.-Y. Lai, W. Huang, *J. Mater. Chem. A* **2016**, *4*, 10493.

[78] A. Lang, J. F. Ponder, A. M. Osterholm, N. J. Kennard, R. H. Bulloch, J. R. Reynolds, *J. Mater. Chem. A* **2017**, *5*, 23887.

[79] D. Khodagholy, M. Gurfinkel, E. Stavrinidou, P. Leleux, T. Herve, S. Sanaur, G. G. Malliaras, *Appl. Phys. Lett.* **2011**, *99*, 163304.

[80] P. Fromherz, *Ann. N. Y. Acad. Sci.* **2006**, *1093*, 143.

[81] S. Inal, G. G. Malliaras, J. Rivnay, *J. Mater. Chem. C* **2016**, *4*, 3942.

[82] J. Rivnay, S. Inal, B. A. Collins, M. Sessolo, E. Stavrinidou, X. Strakosas, C. Tassone, D. M. Delongchamp, G. G. Malliaras, *Nat. Commun.* **2016**, *7*, 11287.

[83] S. Inal, J. Rivnay, A. I. Hofmann, I. Uguz, M. Mumtaz, D. Katsigiannopoulos, C. Brochon, E. Cloutet, G. Hadziioannou, G. G. Malliaras, *J. Polym. Sci., Part B: Polym. Phys.* **2016**, *54*, 147.

[84] J. Rivnay, P. Leleux, M. Ferro, M. Sessolo, A. Williamson, D. A. Koutsouras, D. Khodagholy, M. Ramuz, X. Strakosas, R. M. Owens, C. Benar, J.-M. Badier, C. Bernard, G. G. Malliaras, *Sci. Adv.* **2015**, *1*, e1400251.

[85] S. Inal, J. Rivnay, P. Leleux, M. Ferro, M. Ramuz, J. C. Brendel, M. M. Schmidt, M. Thelakkat, G. G. Malliaras, *Adv. Mater.* **2014**, *26*, 7450.

[86] I. McCulloch, M. Heeney, C. Bailey, K. Genevicius, I. MacDonald, M. Shkunov, D. Sparrowe, S. Tierney, R. Wagner, W. Zhang, M. L. Chabinyc, R. J. Kline, M. D. McGehee, M. F. Toney, *Nat. Mater.* **2006**, *5*, 328.

[87] B. H. Hamadani, D. J. Gundlach, I. McCulloch, M. Heeney, *Appl. Phys. Lett.* **2007**, *91*, 243512.

[88] J. C. Brendel, M. M. Schmidt, G. Hagen, R. Moos, M. Thelakkat, *Chem. Mater.* **2014**, *26*, 1992.

[89] O. Stéphan, P. Schottland, P.-Y. Le Gall, C. Chevrot, C. Mariet, M. Carrier, *J. Electroanal. Chem.* **1998**, *443*, 217.

[90] E. Zeglio, M. M. Schmidt, M. Thelakkat, R. Gabrielsson, N. Solin, O. Inganäs, *Chem. Mater.* **2017**, *29*, 4293.

[91] M. Leclerc, G. Daoust, *Synth. Met.* **1991**, *41*, 529.

[92] T. Johansson, W. Mammo, M. Svensson, M. R. Andersson, O. Inganäs, *J. Mater. Chem.* **2003**, *13*, 1316.

**ADVANCED
SCIENCE NEWS**

www.advancedsciencenews.com

**ADVANCED
FUNCTIONAL
MATERIALS**

www.afm-journal.de

[93] X. Chen, Z. Zhang, Z. Ding, J. Liu, L. Wang, *Angew. Chem.* **2016**, *128*, 10532.

[94] A. Giovannitti, K. J. Thorley, C. B. Nielsen, J. Li, M. J. Donahue, G. G. Malliaras, J. Rivnay, I. McCulloch, *Adv. Funct. Mater.* **2018**, *28*, 1706325.

[95] A. Giovannitti, D.-T. Sbircea, S. Inal, C. B. Nielsen, E. Bandiello, D. A. Hanifi, M. Sessolo, G. G. Malliaras, I. McCulloch, J. Rivnay, *Proc. Natl. Acad. Sci. USA* **2016**, *113*, 12017.

[96] L. R. Savagian, A. M. Österholm, J. F. Ponder Jr., K. J. Barth, J. Rivnay, J. R. Reynolds, *Adv. Mater.* **2018**, 1804647.

[97] R. D. Kimbrough, *Environ. Health Perspect.* **1976**, *14*, 51.

[98] L. A. Estrada, J. J. Deininger, G. D. Kamenov, J. R. Reynolds, *ACS Macro Lett.* **2013**, *2*, 869.

[99] K. M. Persson, R. Karlsson, K. Svennersten, S. Löffler, E. W. H. Jager, A. Richter-Dahlfors, P. Konradsson, M. Berggren, *Adv. Mater.* **2011**, *23*, 4403.

[100] A. Giovannitti, C. B. Nielsen, D.-T. Sbircea, S. Inal, M. Donahue, M. R. Niazi, D. A. Hanifi, A. Amassian, G. G. Malliaras, J. Rivnay, I. McCulloch, *Nat. Commun.* **2016**, *7*, 13066.

[101] A. Giovannitti, I. P. Maria, D. Hanifi, M. J. Donahue, D. Bryant, K. J. Barth, B. E. Makdah, A. Savva, D. Moia, M. Zetek, P. R. F. Barnes, O. G. Reid, S. Inal, G. Rumbles, G. G. Malliaras, J. Nelson, J. Rivnay, I. McCulloch, *Chem. Mater.* **2018**, *30*, 2945.

[102] H. Sun, M. Vagin, S. Wang, X. Crispin, R. Forchheimer, M. Berggren, S. Fabiano, *Adv. Mater.* **2018**, *30*, 1704916.

[103] S. Wang, H. Sun, U. Ail, M. Vagin, P. O. Å. Persson, J. W. Andreasen, W. Thiel, M. Berggren, X. Crispin, D. Fazzi, S. Fabiano, *Adv. Mater.* **2016**, *28*, 10764.

[104] R. A. Schlitz, F. G. Brunetti, A. M. Glaudell, P. L. Miller, M. A. Brady, C. J. Takacs, C. J. Hawker, M. L. Chabinyc, *Adv. Mater.* **2014**, *26*, 2825.

[105] B. D. Naab, X. Gu, T. Kurosawa, J. W. F. To, A. Salleo, Z. Bao, *Adv. Electron. Mater.* **2016**, *2*, 1600004.

[106] D. M. de Leeuw, M. M. J. Simenon, A. R. Brown, R. E. F. Einerhand, *Synth. Met.* **1997**, *87*, 53.

[107] L. Sigg, in *Redox: Fundamentals, Processes and Applications* (Eds: J. Schüring, H. D. Schulz, W. R. Fischer, J. Böttcher, W. H. M. Duijnisveld), Springer, Berlin **2000**, p. 1.

[108] J. A. Kerszulis, K. E. Johnson, M. Kuepfert, D. Khoshabo, A. L. Dyer, J. R. Reynolds, *J. Mater. Chem. C* **2015**, *3*, 3211.

[109] J. F. Ponder, A. M. Österholm, J. R. Reynolds, *Macromolecules* **2016**, *49*, 2106.

[110] K. Cao, D. E. Shen, A. M. Österholm, J. A. Kerszulis, J. R. Reynolds, *Macromolecules* **2016**, *49*, 8498.

[111] J. F. Ponder, B. Schmatz, J. L. Hernandez, J. R. Reynolds, *J. Mater. Chem. C* **2018**, *6*, 1064.

[112] G. Conboy, H. J. Spencer, E. Angioni, A. L. Kanibolotsky, N. J. Findlay, S. J. Coles, C. Wilson, M. B. Pitak, C. Risko, V. Coropceanu, J.-L. Bredas, P. J. Skabara, *Mater. Horiz.* **2016**, *3*, 333.

[113] N. E. Jackson, B. M. Savoie, K. L. Kohlstedt, M. Olvera de la Cruz, G. C. Schatz, L. X. Chen, M. A. Ratner, *J. Am. Chem. Soc.* **2013**, *135*, 10475.

[114] D. J. Pascoe, K. B. Ling, S. L. Cockroft, *J. Am. Chem. Soc.* **2017**, *139*, 15160.

[115] H. Yan, Z. Chen, Y. Zheng, C. Newman, J. R. Quinn, F. Dötz, M. Kastler, A. Facchetti, *Nature* **2009**, *457*, 679.

[116] L. Q. Flagg, R. Giridharagopal, J. Guo, D. S. Ginger, *Chem. Mater.* **2018**, *30*, 5380.

[117] A. Savva, S. Wustoni, S. Inal, *J. Mater. Chem. C* **2018**, *6*, 5218.

[118] C. K. Lo, C.-Y. Wang, S. D. Oosterhout, Z. Zheng, X. Yi, C. Fuentes-Hernandez, F. So, V. Coropceanu, J.-L. Brédas, M. F. Toney, B. Kippelen, J. R. Reynolds, *ACS Appl. Mater. Interfaces* **2018**, *10*, 11995.

[119] W. Du, D. Ohayon, C. Combe, L. Mottier, I. P. Maria, R. S. Ashraf, H. Fiumelli, S. Inal, I. McCulloch, *Chem. Mater.* **2018**, *30*, 6164.

[120] J. F. Ponder, A. M. Österholm, J. R. Reynolds, *Chem. Mater.* **2017**, *29*, 4385.